Optical Spectra Observed during Ion-Molecule Collisions Using Low-Energy N_2^+ and Ar^+ Beams*

Chelcie Liu and H. P. Broida†
Department of Physics, University of California, Santa Barbara, California 93106
(Received 7 May 1970)

A survey has shown that light emission from low-energy (< 1 keV) ion-molecule reactions is a common occurrence. Ar^+ and N_2^+ were used with target gases of Ar, H_2, D_2, CO, N_2, O_2, NO, N_2O, CO_2, CH_4, and C_2H_2; in addition, He, Ne, and Kr were used as N_2^+ targets. Electronically excited states were produced by charge transfer and ionization with simultaneous excitation, conversion of translational to electronic energy of the incident ion or target, and dissociation with simultaneous excitation. For several collision partners, more than one of these reactions was seen. In general, charge-transfer reactions had the largest cross sections, to 2×10^{-16} cm^2, for ion laboratory energies of several hundred eV. Cross sections for the strongest features in the other types of reactions were about $(1-5)\times10^{-17}$ cm^2.

INTRODUCTION

One of the principal energy-loss mechanisms of heavy particles passing through matter is the excitation of atomic and molecular states. Presently, however, only a small amount of experimental information on excitation produced by low-energy (< 1 keV) ion-molecule reactions has been obtained from ion-beam studies.[1-18] Therefore, a survey has been made at energies below 1 keV to find (i) which ion-target combinations lead to photon emission, (ii) what types of reactions lead to excited states, and (iii) cross sections for these reactions.

Ar^+ and N_2^+ were the ions used. Target gases for both ions included Ar, H_2, D_2, CO, N_2, O_2, NO, N_2O, CO_2, CH_4, and C_2H_2; in addition, He, Ne, and Kr were used as N_2^+ targets.

APPARATUS

The electron impact ion source and lens system used were previously developed by Utterback and Miller.[19] The gas to be ionized (G_I, Fig. 1) entered through the anode and was kept at pressures (P_I) of approximately 0.05 Torr. To help keep the ion source free from contamination, the gas to be ionized was passed through a liquid-nitrogen trap. 20–40-eV electrons were used to produce N_2^+ beams, while 28–40-eV electrons were used to produce Ar^+ beams.

Ions were extracted through a 0.25-mm hole into an electrostatic lens system. The final energy of the beam was determined by the third lens at the end of the gun. As ions left the gun, they passed through two sets of mutually perpendicular parallel-plate capacitors which were used to make small adjustments in the final beam direction.

The target chamber consisted of a quartz cylinder with a length of 32 mm, inner diameter of 30 mm, and walls of 1.8 mm sandwiched between two metal plates. The ion beam entered this chamber through a hole in the top plate 2.5 mm in diameter and 6.35 mm long. That portion of the ion current which entered the target chamber depended on the ion and its final energy. At laboratory energies of several hundred eV, the current into the target chamber for both ions was approximately 0.1 μA. Target-chamber currents were measured by grounding the top plate of the target chamber and connecting the bottom plate to a calibrated picoammeter.

Secondary electrons were 0.2 and 0.15 of the measured beam current for ion energies of 880 and 740 eV, respectively. No corrections were made at

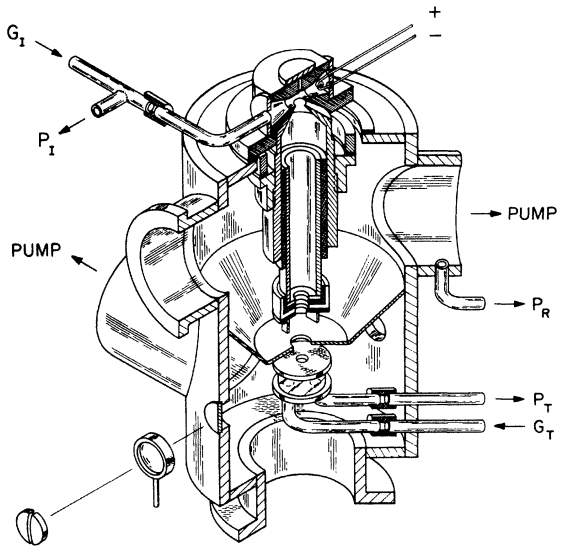

FIG. 1. Ion gun and vacuum system. G_I, gas to be ionized; P_I, ion-source pressure monitor; P_R, reference pressure for capacitance manometer; P_T, target-gas pressure monitor; G_T, target-gas inlet.

energies below 600 eV. Because of the difficulty in determining the secondary electron coefficients, the error in the beam current measurement may be as much as 10–15% at the high beam energies. It is probably less than 5% for ion energies below 300 eV.

The fact that significant changes were observed in the cross sections for some of the reactions when the ion energy was changed by a few eV indicated that the energy half-width of the ion beam was a few eV or less. This is consistent with the measurement of an ion energy spread in this type of ion gun of 0.5 eV for 35-eV N_2^+.[19] The ion beam was not magnetically analyzed because the previous work of Utterback[20] had shown the amount of ion-beam contamination to be small; N_2 and Ar used in the ion source were quoted to be 99.99% N_2 and 99.999% Ar by the vendor.

Target gases (G_T, Fig. 1) were introduced into the target chamber through a hole in the bottom plate. The other connection in the bottom plate led to an absolute capacitance manometer which was used to measure the target pressure (P_T). For a relatively high target-chamber pressure of 10^{-2} Torr, the pressure in the volume surrounding the target chamber was 10^{-4} Torr, while that in the ion-gun region was 10^{-5} Torr.

Light emitted from the reaction region passed through a quartz port where it was collected by a lens and focused on the entrance slit of an $f/6.8$, $\frac{3}{4}$-m, Czerny-Turner scanning grating monochromator capable of 0.1-Å resolution. The wavelength readout of the spectrometer was calibrated to within ±1 Å over the spectral region covered in the scans. Unfortunately, because of a small variation in the spectrometer's scan speed and the low resolution, uncertainties in measured wavelengths were some-

TABLE I. Observed spectra between 2500 and 5500 Å. Cross sections σ measured at 900 eV.

Target	N_2^+ Spectral system		σ (10^{-18} cm^2)	Ar^+ Spectral system		σ (10^{-18} cm^2)
H_2	N_2^+	$B\,^2\Sigma_u^+ - X\,^2\Sigma_g^+$	20	H Balmer		1
	H Balmer		2			
D_2	N_2^+	$B\,^2\Sigma_u^+ - X\,^2\Sigma_g^+$	20	D Balmer		2
	D Balmer		2			
CO	CO^+	$A\,^2\Pi_i - X\,^2\Sigma^+$	210	CO^+	$A\,^2\Pi_i - X\,^2\Sigma^+$	150
	N_2^+	$B\,^2\Sigma_u^+ - X\,^2\Sigma_g^+$	10			
N_2	N_2^+	$B\,^2\Sigma_u^+ - X\,^2\Sigma_g^+$	40	N_2^+	$B\,^2\Sigma_u^+ - X\,^2\Sigma_g^+$	20
	N I	$3s\,^2P - 3P'\,^2D^0$(?)		N_2	$C\,^3\Pi_u - B\,^3\Pi_g$(?)	
	N_2	$C\,^3\Pi_u - B\,^3\Pi_g$(?)		Ar I	(?)	
O_2	N_2^+	$B\,^2\Sigma_u^+ - X\,^2\Sigma_g^+$	15	O I	$3^3S^0 - 4\,^3P$(?)	
	O I	$3^5S^0 - 4\,^5P$	1			
	O I	$3^3S^0 - 4\,^3P$	1			
NO-N_2O	N_2O^+	$\tilde{A}\,^2\Sigma^+ - \tilde{X}^2\Pi_i$	100	N_2O^+	$\tilde{A}\,^2\Sigma^+ - \tilde{X}^2\Pi_i$	50
	N_2^+	$B\,^2\Sigma_u^+ - X\,^2\Sigma_g^+$	10			
CO_2	CO_2^+	$\tilde{A}\,^2\Pi_u - \tilde{X}\,^2\Pi_g$	120	CO_2^+	$\tilde{A}\,^2\Pi_u - \tilde{X}\,^2\Pi_g$	15
	CO_2^+	$\tilde{B}\,^2\Sigma_u^+ - \tilde{X}\,^2\Pi_g$	6	CO_2^+	$\tilde{B}\,^2\Sigma_u^+ - \tilde{X}\,^2\Pi_g$	2
	N_2^+	$B\,^2\Sigma_u^+ - X\,^2\Sigma_g^+$(?)				
CH_4	N_2^+	$B\,^2\Sigma_u^+ - X\,^2\Sigma_g^+$	10	CH	$A\,^2\Delta - X\,^2\Pi$	4
	CH	$A\,^2\Delta - X\,^2\Pi$	6	H Balmer		4
	H Balmer			CH	$B\,^2\Sigma^- - X\,^2\Pi$	1
	CH	$B\,^2\Sigma^- - X\,^2\Pi$	1			
	N_2	$C\,^3\Pi_u - B\,^3\Pi_g$(?)				
C_2H_2	CH	$A\,^2\Delta - X\,^2\Pi$	15	CH	$A^2\Delta - X\,^2\Pi$	20
	CH	$B\,^2\Sigma^- - X\,^2\Pi$	4	CH	$B\,^2\Sigma^- - X\,^2\Pi$	5
	H Balmer		1	H Balmer		2
	C_2	$A\,^3\Pi_g - X\,^3\Pi_u$	1			
	N_2^+	$B\,^2\Sigma_u^+ - X\,^2\Sigma_g^+$				
	N_2	$C\,^3\Pi_u - B\,^3\Pi_g$(?)				
	C_2	$c\,^1\Pi_g - b\,^1\Pi_u$(?)				
He	N_2^+	$B\,^2\Sigma_u^+ - X\,^2\Sigma_g^+$	30			
Ne	N_2^+	$B\,^2\Sigma_u^+ - X\,^2\Sigma_g^+$	20			
	N I	$3s\,^2P - 3P'\,^2D^0$(?)				
Ar	N_2^+	$B\,^2\Sigma_u^+ - X\,^2\Sigma_g^+$	30	Ar I		
	Ar I			Ar II		
Kr	N_2^+	$B\,^2\Sigma_u^+ - X\,^2\Sigma_g^+$	40			
	Kr I		4			
	Kr II					

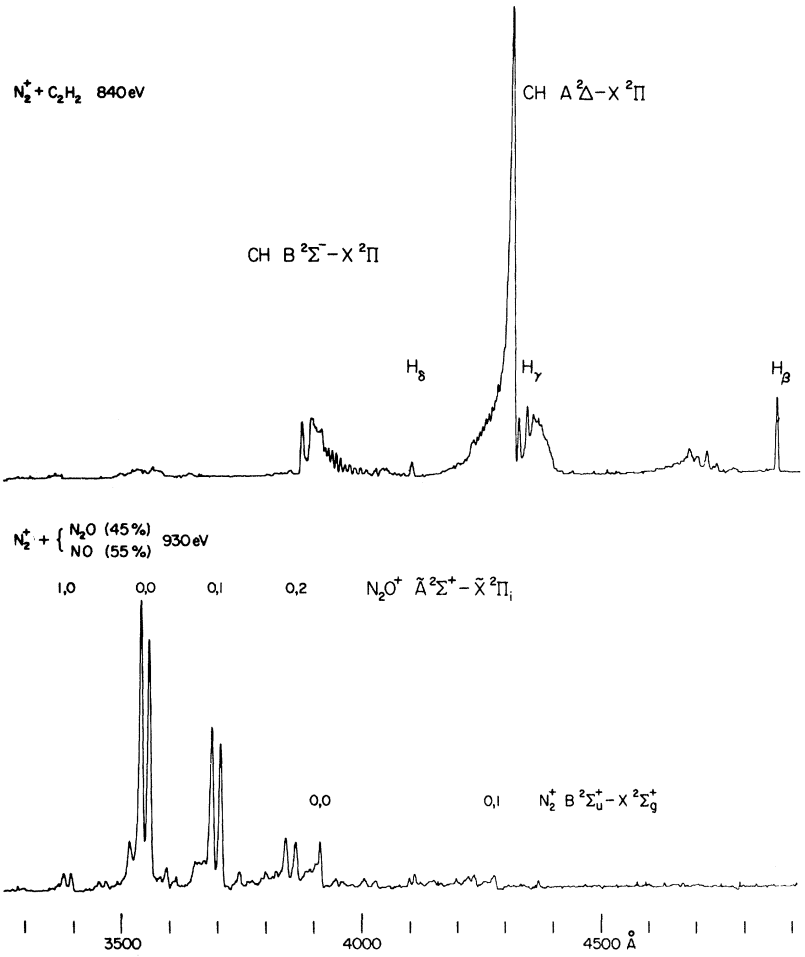

FIG. 2. 5-Å resolution spectra observed when C_2H_2 and a NO-N_2O mixture were bombarded by 840- and 930-eV N_2^+. In the C_2H_2 spectrum, the unlabeled feature at 4700 Å is due to C_2 and the feature at 3914 Å superimposed on the CH transition as well as most of the weak feature between 3500 and 3600 Å are due to the N_2^+ first-negative system.

times as high as ± 5 Å. Spectra were obtained with a photomultiplier–dc-amplifier–pen–recorder combination. After the spectra were recorded, the spectrometer–collecting-lens combination was calibrated with a quartz-iodine standard lamp.

SPECTROSCOPIC OBSERVATIONS

Photon emission in the visible and near-ultraviolet regions of the spectrum was found to be a common occurrence for ion-molecule reactions below 1 keV. Only in the reactions $Ar^+ + O_2$ and NO, and possibly $N_2^+ + NO$, was the emitted light too weak to analyze. The results of the reaction $N_2^+ + NO$ were ambiguous because the NO cylinder used was found to contain approximately 45% N_2O.

Several different types of reactions have been found which lead to electronically, vibrationally, and rotationally excited states: Charge transfer can lead directly to excited states of the target, dissociation with simultaneous excitation may occur, and translational energy can be converted to electronic energy of the target or projectile molecule. At higher energies, part of the light emission in reactions which have been identified as charge transfer with simultaneous excitation could have been due to ionization with excitation. Because charge transfer would require less energy than ionization, it seems reasonable to assume that the majority of the light was from charge-transfer reactions. However, as will be discussed later, it was found that relative intensities of spectral features observed for a given reaction could not be estimated from the relative amounts of energy required to produce the features.

Principal spectra observed and the wavelength region surveyed for each reaction are summarized in Table I. Tentative identifications are indicated by a question mark. Table I also contains approximate cross sections for production of that portion of the spectral system which falls in the wavelength region surveyed, for each reaction where a meaningful estimate of this cross section could be made. Spectra used for these estimates were obtained using ions with a laboratory energy of 900 eV. In many cases, these estimates probably are accurate only to a factor of 2 or 3, but some cross sections were measured to within 50%. Examples of observed spectra are shown in Figs. 2–5.

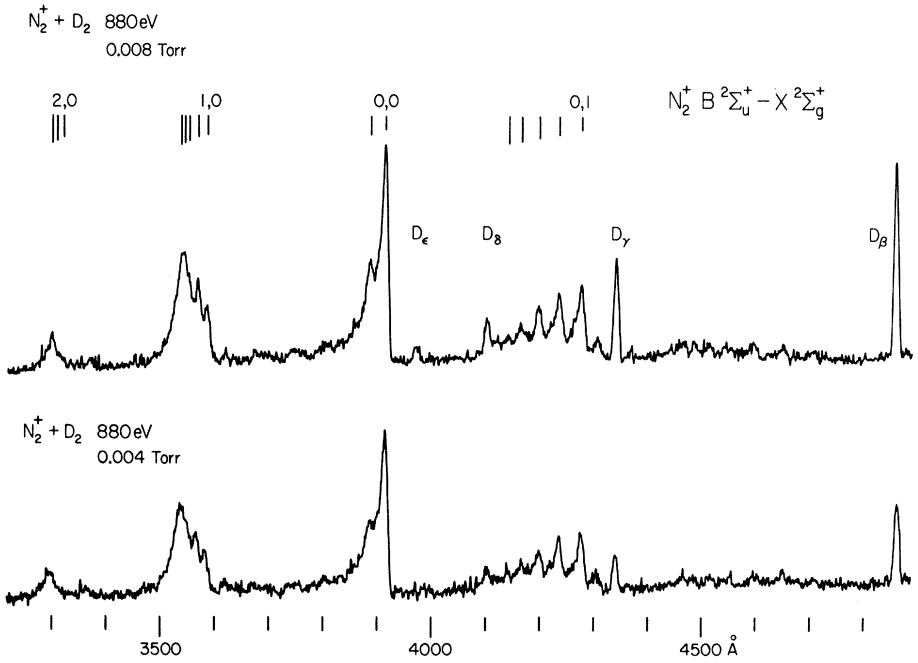

FIG. 3. 10-Å resolution spectra of the N_2^+ first-negative system and the D Balmer series observed when D_2 at 0.004 and 0.008 Torr was bombarded by 880-eV N_2^+.

Since previous observers[15,21,22] have found that polarized light is emitted during some ion-molecule reactions, a preliminary check of polarization characteristics of the emitted radiation for two of the reactions was made. The 0, 1 band of the N_2^+ first-negative system at 4278 Å from the reaction $N_2^+ + N_2$, and the CH–4300-Å system from the reaction $N_2^+ + C_2H_2$ were checked for an N_2^+ laboratory energy of 900 eV. In these two reactions the emitted light was found to be either unpolarized or slightly polarized parallel to the ion beam.

Usually an electron accelerating voltage of at least 28 V was required to produce strong N_2^+ or Ar^+ beams. Other workers,[23] using an ion gun similar to the one used here, have found evidence for the existence of long-lived excited N_2^+ ions in the beam when the electron bombarding energy was above 22 eV. Therefore, an attempt was made to determine what effect ions in metastable electronic states had on the observed spectra by comparing spectra obtained with N_2^+ beams produced by 20- and and 40-eV electrons and Ar^+ beams produced by 28- and 40-eV electrons. The reactions for which this was done were N_2^+ colliding with He, H_2, N_2, CO,

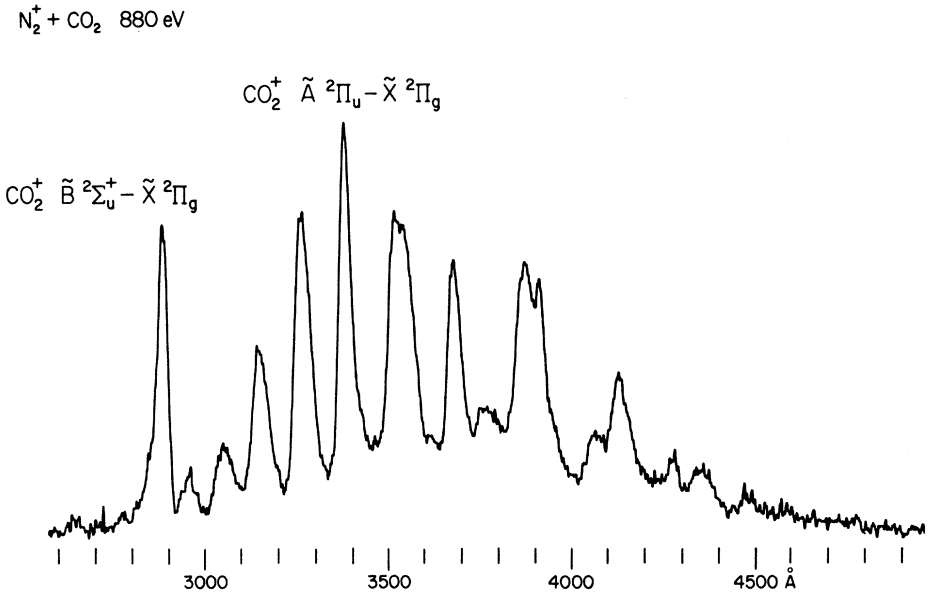

FIG. 4. 20-Å resolution spectrum of the $CO_2^+ \tilde{A}\,^2\Pi_u - X\,^2\Pi_g$ and $\tilde{B}\,^2\Sigma_u^+ - \tilde{X}\,^2\Pi_g$ transitions observed when CO_2 was bombarded by 880-eV N_2^+. The peak at 3910 Å is the 0, 0 band of the $N_2^+ B\,^2\Sigma_u^+ - X\,^2\Sigma_g^+$ transition.

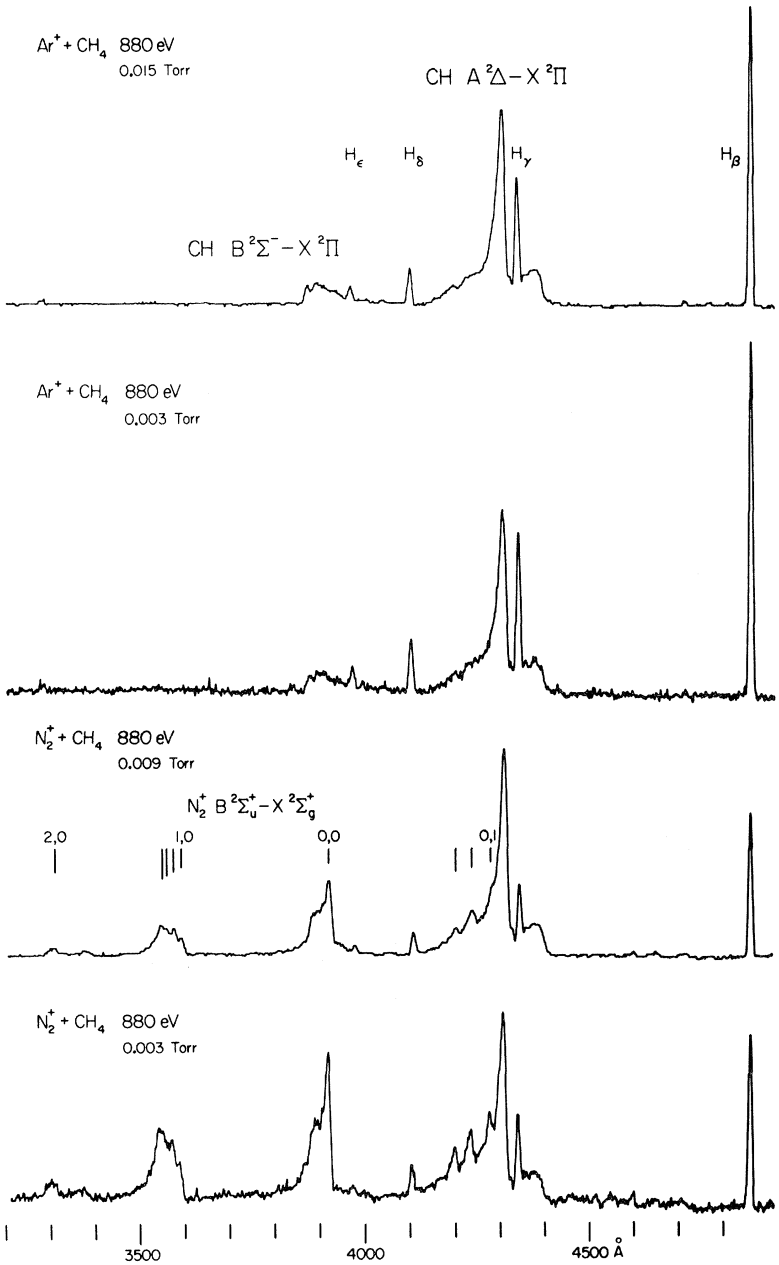

FIG. 5. 10-Å resolution spectra showing the CH $A\,^2\Delta - X\,^2\Pi$ transition, the CH $B\,^2\Sigma^- - X\,^2\Pi$ transition and the H Balmer series observed when 880-eV N_2^+ and Ar^+ bombarded CH_4 at various pressures. In the N_2^+ reactions, the N_2^+ first-negative system was also observed.

and C_2H_2; and Ar^+ colliding with D_2 at several center-of-mass energies. In some cases, the reactions involving the beams formed by the low-energy electrons appeared a few percent brighter. Therefore, it appears that long-lived excited N_2^+ ions had little, if any, effect on the observed spectra at relatively large center-of-mass energies. In contrast, some preliminary phototube measurements of the total light emitted between 3000 and 6000 Å for the reactions Ar^+ and N_2^+ with C_2H_2 indicated that, for center-of-mass energies of a few eV, reactions with ions produced by the 40-eV electrons had about four times and two times as much light for the Ar^+ and N_2^+ reactions, respectively, than reactions using ions produced by low-energy electrons.

CROSS SECTIONS

Cross sections measured in these experiments were those for the production of various spectral features, such as a vibrational band, spectral line, or vibrational band sequence. Cross sections for a complete spectral system, such as the CO^+ comet-tail bands, could then be obtained by summing the cross sections for all spectral features in that system. If there were no higher-lying excited states which cascaded into the electronic state from which the spectral system under study originated, and no other mechanism by which this excited state could

decay, the cross section for formation of the spectral system would be the same as the cross section for formation of the excited state.

If a beam of I_0 particles per second is incident normally on a semi-infinite medium containing n stationary target particles per cm^3, the number of photons dN per second produced at a depth x as the beam travels a distance dx through the target gas is given by the equation

$$dN = \sigma_p n I_0 \exp - \sigma_T n x \, dx, \tag{1}$$

where σ_p is the cross section for the reaction leading to photon emission and σ_T is the sum of the cross sections for all processes which remove ions from the beam. The total number N of photons produced in a second as the beam penetrates the target material to a depth L is therefore given by the equation

$$N = \sigma_p I_0 [1 - \exp(-\sigma_T n L)]/\sigma_T . \tag{2}$$

If "thin-target" or "single-collision" conditions exist, i.e., if the product $\sigma_T n L \ll 1$, the exponential can be expanded in a series and we have

$$N = \sigma_p I_0 n L. \tag{3}$$

As long as thin-target conditions prevail, Eq. (3) is valid, and the number of photons emitted increases linearly with pressure. It should be noted that if thin-target conditions are not maintained, the number of photons produced in secondary collisions may become comparable to the number produced in primary collisions.

To determine σ_p, the quantities N, I_0, n, and L had to be measured. L was determined from the length of the slit which was illuminated, I_0 from the ion current measured when the target pressure was zero, and n from the target pressure. N, the number of photons emitted per second at a given wavelength, was determined by comparing spectra of light from the reaction region with spectra of a calibrated source.[18]

The cross sections for production of extensive band systems, e.g., the CO^+ comet-tail system, were determined by summing the cross sections which had been calculated for each individual band. Because of the wavelength response characteristics of the spectrometer, some CO^+ vibrational bands were not observed which originated from vibrational levels for which other bands were observed. A 15% increase in the cross-section measurements was made to correct for strong unobserved bands (0, 2; 0, 3; 1, 2; 2, 3; 2, 4; and 3, 5) using the transition probabilities calculated by Jain and Sahni.[24]

Since, at low beam energies, it was difficult to obtain resolved spectra because of decreasing beam currents and cross sections, either a bare phototube

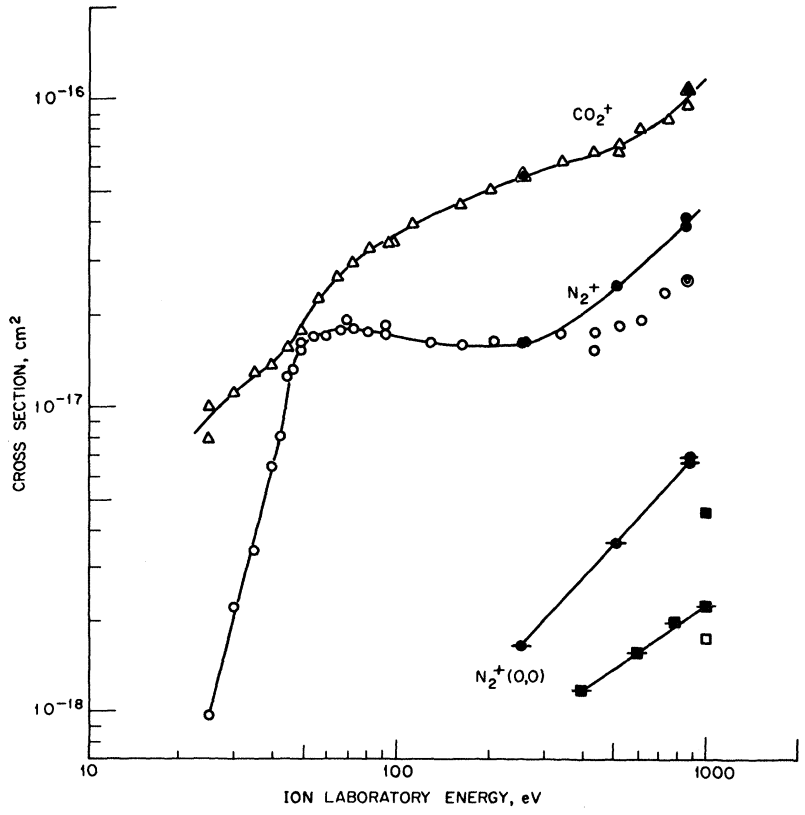

FIG. 6. Cross sections as a function of N_2^+ laboratory energy for the production of the $N_2^+ B\,^2\Sigma_u^+ - X\,^2\Sigma_g^+$ transition in the reaction $N_2^+ + N_2$ (phototube, ○; spectrometer, ●) and the $CO_2^+ \tilde{A}\,^2\Pi_u - \tilde{X}\,^2\Pi_g$ transition in the reaction $N_2^+ + CO_2$ (phototube, △; spectrometer, ▲). Cross sections as a function of N_2^+ laboratory energy for the production of the $N_2^+ B\,^2\Sigma_u^+ - X\,^2\Sigma_g^+ 0,0$ band (-●-) are shown and compared to the results of Neff and Carleton (Refs. 1, 16) (-■-) and Doering (Ref. 25) (□, original; ■ , corrected).

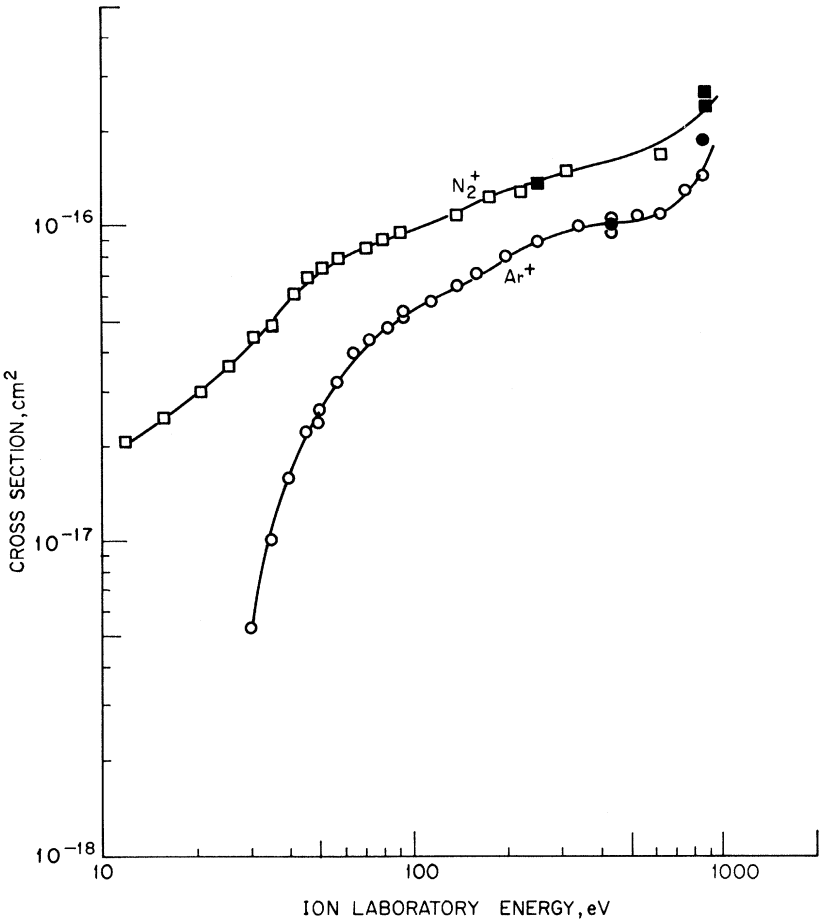

FIG. 7. Cross sections as a function of ion laboratory energy for production of the $CO^+ A\,^2\Pi_i - X\,^2\Sigma^+$ transition in the reactions $Ar^+ + CO$ (phototube, ○; spectrometer, ●) and $N_2^+ + CO$ (phototube, □; spectrometer, ■).

or a phototube in combination with a narrow-band interference filter was used to detect the emitted light used in the cross-section measurements. Because of its simplicity, this technique also was used at high energies. In addition, lower target pressures could be used for the phototube measurements, increasing the validity of the thin-target approximation. Most of the phototube data were obtained with target pressures between $(4-6)\times10^{-4}$ Torr. Target pressures used for the spectrometer measurements ranged from $(1.5-2.5)\times10^{-3}$ Torr. Phototube cross sections were normalized to cross sections measured using the integrated intensity of the resolved band system. An interference filter with a peak transmission at 4280 Å and a half-width of 200 Å was used for the CH–4300-Å system.

It was thus tacitly assumed that the relative intensities of the various bands of the electronic transition either changed very little over the energy range for which the bare phototube measurements were made, or the response of the phototube was fairly flat over the region where there were changes in relative intensity. Large changes in the relative intensities of the vibrational bands of the N_2^+ first-negative system excited in the reaction $N_2^+ + N_2$ were observed when the energy of the incident N_2^+ was changed. These changes in relative intensity, coupled with the fact that the quantum efficiency of the phototube used in the bare phototube measurements varied over the wavelength region in which the N_2^+ first-negative system was observed, probably account for some of the deviation between the cross sections determined by these two methods (Fig. 6).

Deviations between the cross sections determined by the two methods also would have occurred if the relative intensities of the spectral features of interest and other spectral features in the wavelength region for which the phototube was sensitive changed from the values they had at the energy where the phototube cross sections were normalized. This, too, was a problem in the $N_2^+ + N_2$ reaction. At 880 eV, about 20% of the photons emitted between 3000 and 5000 Å in this reaction were not from the N_2^+ first-negative system. The fraction increased to 30% when the energy of the incident N_2^+ was reduced to 255 eV. Because of these two possibilities for deviations between the cross sections determined by the two methods in the $N_2^+ + N_2$ reaction, when there was a choice the curve was drawn

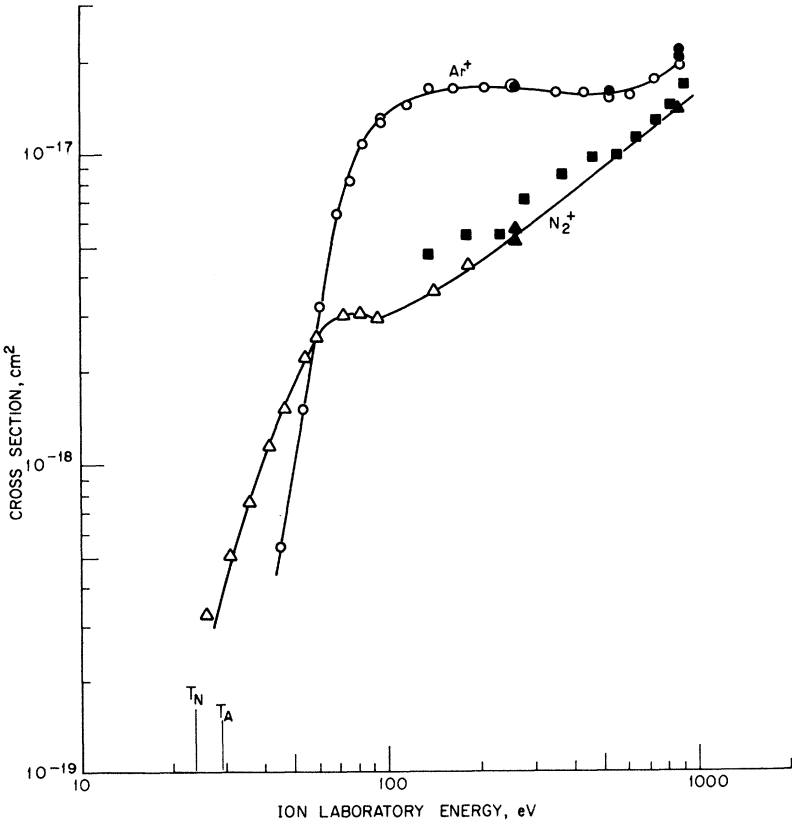

FIG. 8. Cross sections as a function of ion laboratory energy for production of the CH $A\,^2\Delta$–$X\,^2\Pi$ transition in the reactions $Ar^+ + C_2H_2$ (phototube, ○; spectrometer, ●) and $N_2^+ + C_2H_2$ (phototube, △; different spectrometer calibrations ▲, ■). Threshold laboratory energies for production of the CH $A\,^2\Delta$ state in the $N_2^+ + C_2H_2$ and $Ar^+ + C_2H_2$ reactions are designated by T_N and T_A, respectively.

through the points determined using the integrated intensity instead of averaging in the phototube cross sections.

To check the accuracy of the techniques used, the cross section for production of the 0, 0 band (3914 Å) of the N_2^+ first-negative system in the reaction $N_2^+ + N_2$ was measured and compared to the values published by Neff and Carleton,[1,16] and Doering[25] (Fig. 6). Only the area of the 0, 0 sequence from the edge of the 0, 0 band to the edge of the 1, 1 band was used in the calculation of the cross sections for production of the N_2^+–3914-Å band shown in Fig. 6 because this most closely matched the techniques described by Doering[25] and Neff.[1] Had light from the entire $\Delta v = 0$ sequence been used, the calculated cross sections would have been 1.5 times as large.

Doering calibrated his apparatus by observing the N_2^+–3914-Å emission from the bombardment of N_2 by 180-eV electrons. He took the cross section for this reaction to be 5.3×10^{-18} cm^2, based on the work of Stewart,[26] and that of Sheridan, Oldenberg and Carleton.[27] Recent work[28–31] has shown that the cross section for this reaction is 1.4×10^{-17} cm^2. Therefore, the cross-section values published by Doering should be multiplied by a factor of 2.6 to make them consistent with the best cross-section data for electron excitation. This corrected cross section also is shown in Fig. 6.

Neff[1] determined his absolute-emission cross sections by extrapolating the results of Sluyters and Kistemaker[32] and adjusting the relative cross sections for other processes to conform to these values. He also made a direct measurement of the absolute-emission cross section for production of the 0, 0 band of the N_2^+ first-negative system in the reaction $N_2^+ + N_2$. The directly measured cross section was 30% higher than the cross section obtained indirectly. Neff felt that his cross-section measurements were accurate to within 50% and were probably on the low side.

In this work, the measurements of pressure and path length observed were probably accurate to ± 5%.[18] Error in the beam-current measurement may have been as much as 10–15% at high beam energies, but was probably less than 5% for ion energies below 300 eV. The over-all accuracy of the final calibration of the spectometer was estimated to be ± 30%. Thus, the final cross-section measurements should have been accurate to ± 50%. Since Neff believed that his values were low, his own work indicating 30% low, the disagreement between the cross sections for production of the 0, 0 band of the N_2^+ first-negative system measured here and those measured previously is not unreasonable. Figure 6 also shows cross sections, as a function of energy, for production of the entire N_2^+ $B\,^2\Sigma_u^+$–$X\,^2\Sigma_g^+$ system.

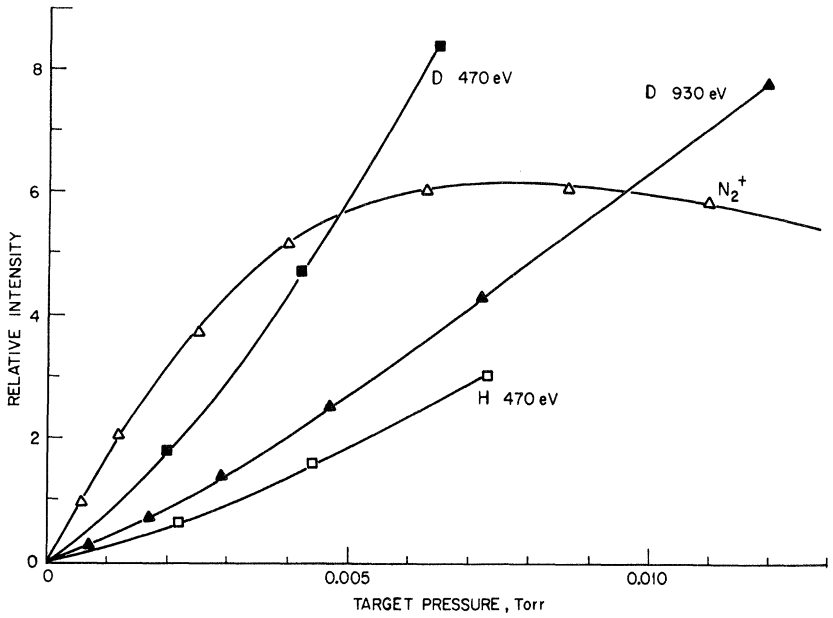

FIG. 9. Relative intensities of the H Balmer β lines as a function of target pressure for the reactions $N_2^+ + D_2$ (930 eV, ▲; 470 eV, ■) and $N_2^+ + H_2$ (470 eV, □), and relative intensity of the $N_2^+ B\,^2\Sigma_u^+ - X\,^2\Sigma_g^+$ 0, 0 band as a function of H_2 pressure for the reaction $N_2^+ + H_2$ (930 eV, △). The relative intensity of one curve with respect to another is not significant.

Cross sections as a function of energy for production of the $CO_2^+ \tilde{A}\,^2\Pi_u - \tilde{X}\,^2\Pi_g$ system in the reaction $N_2^+ + CO_2$ (Fig. 6), the $CO^+ A\,^2\Pi_i - X\,^2\Sigma^+$ system in the reactions N_2^+ and $Ar^+ + CO$ (Fig. 7), and the CH $A\,^2\Delta - X\,^2\Pi$ system in the reactions N_2^+ and $Ar^+ + C_2H_2$ (Fig. 8) also were measured. Additional cross sections given in Table I were obtained by visual estimates of spectra obtained with 900-eV beams. The phototube measurements (△) for the reaction $N_2^+ + C_2H_2$ (Fig. 8) were normalized to the cross-section measurements obtained using the spectrometer (▲) by extrapolating the spectrometer measurements. To obtain an indication of the validity of this extrapolation, cross sections obtained using the initial calibration of the apparatus (■) were plotted even though the accuracy was not as high.

From Figs. 6–8, it can be seen that the cross sections generally decreased with decreasing energy below 1000 eV, but that this decrease was not uniform. Plateaus were observed in the cross-section–versus–energy curve for three of the six reactions. Part of the reason for the plateau in the $N_2^+ + N_2$ cross-section curve (Fig. 6) is that the intensity of spectral features other than the N_2^+ first-negative system increased as the energy of the in-

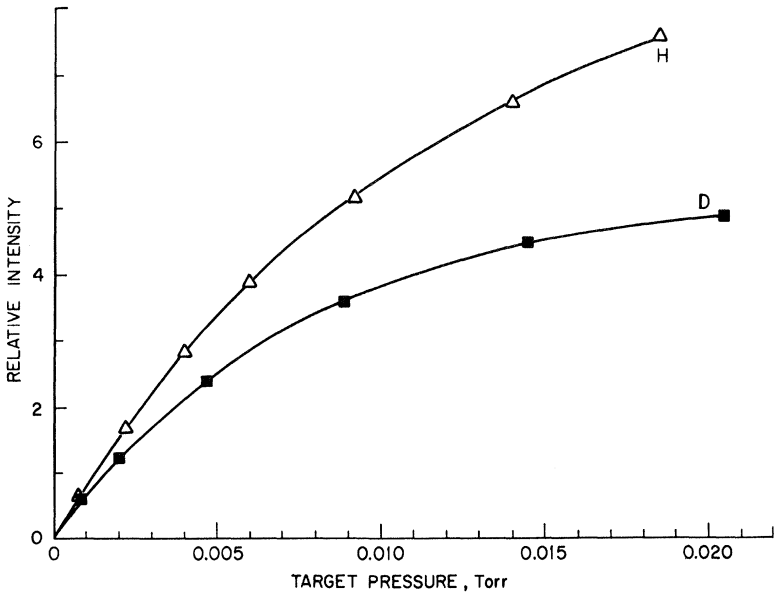

FIG. 10. Relative intensities of the H Balmer β lines as a function of target pressure for the reactions $Ar^+ + H_2$ (930 eV, △) and $Ar^+ + D_2$ (470 eV, ■). The relative intensity of one curve with respect to another is not significant.

cident N_2^+ decreased, compensating for the decrease in the N_2^+ emission. Cross sections for the production of some weak unidentified features in the reactions Ar^+ and $N_2^+ + O_2$, $N_2^+ + He$ and $N_2^+ + CH_4$ also increased as the ion energy was decreased. Other observers[5,6] have noted local maxima in cross sections for other reactions in this energy range. One of the most interesting features of the cross-section curves was the rapid rise in the cross section with increasing ion energy after the threshold energy had been reached.

It was found that the relative intensities of spectral features observed for a given reaction could not be estimated from the relative amounts of energy required to produce the features. In many reactions where N_2^+ was the incident ion, the N_2^+ first-negative system was the dominant spectral system (e.g., the N_2^+–rare-gas reactions). However, in other reactions (e.g., $N_2^+ + C_2H_2$) the N_2^+ first-negative system was much weaker than spectral systems which required much more energy for their production.

Because an adequate theoretical description of the excitation processes studied here does not exist, there are no theoretical predictions with which a quantitative comparison of the measured cross sections can be made.

PRESSURE DEPENDENCE

In order to obtain more information about the excitation mechanism and other processes taking place in the target chamber, the light intensity as a function of target pressure was measured. From this type of measurement, it was possible to determine at what pressures deviations from the thin-target approximation became important for a given set of collision partners. Also, an indication of the importance of collisional deexcitation could be obtained by noting at what pressure the intensity of the emitted light started to decrease with increasing pressure.

The intensity of the N_2^+ emission from the reactions $N_2^+ + H_2$ and $N_2^+ + D_2$ increased linearly at first, gradually reached a maximum, and then declined as the target pressure was increased (Fig. 9). In contrast, the intensity of the H Balmer lines in the same reactions increased at a rate which was greater than linear but not quadratic at low pressures, and tended toward a linear increase with increasing target pressures at high pressures. Therefore, the Balmer emission from the reactions $N_2^+ + H_2$ and $N_2^+ + D_2$ not only behaved much differently from the N_2^+ emission when the pressure was changed, but also much differently from the Balmer emission in the reactions $Ar^+ + H_2$ and $Ar^+ + D_2$ (Fig. 10). Since the variation in hydrogen intensity with pressure changes was less than quadratic but greater than linear, there may have been two different processes which led to excited hydrogen atoms. One process could involve a direct interaction of the ion beam with the target, as was the case in the $Ar^+ + H_2$ and $Ar^+ + D_2$ reactions, while the other could involve an interaction of the target with an electron or atom formed in a previous ion-target collision.

Because of the different pressure dependence of the N_2^+ and H (D) emission in the reaction $N_2^+ + H_2$ (D_2), the relative intensities of the N_2^+ and H (D) emission varied with the H_2 (D_2) target pressure (Fig. 3). The relative intensity of the CH and H emission in the reaction $Ar^+ + CH_4$ (Fig. 5), the CH, H, and N_2^+ emission in the reaction $N_2^+ + CH_4$ (Fig. 5), and the Ar and N_2^+ emission in the reaction $N_2^+ + Ar$ also were found to vary with the pressure of the target. Detailed studies of this type were not made for other reactions. Differences in the intensity variation with pressure of the different species excited in a given reaction could be due to differences in the importance of collisional deexcitation for the species as well as differences in their formation mechanism. If one of the excited species had a lower collision rate, and/or shorter lifetime, or just a lower efficiency for converting electronic into kinetic energy during the collision, its intensity would increase relative to that of the other species, even if there were no differences in the formation mechanisms of the various excited species.

---

*Work supported in part by the U.S. Air Force Office of Scientific Research Office of Aerospace Research, under Grant No. AFOSR-70-1851.

†Visiting Fellow at the Joint Institute of Laboratory Astrophysics, University of Colorado, Boulder, Colo. (June 1969–September 1970).

[1]S. H. Neff, Astrophys. J. 140, 348 (1964).

[2]R. F. Stebbings, R. A. Young, C. L. Oxley, and H. Ehrhardt, Phys. Rev. 138, A1312 (1965).

[3]N. G. Utterback and H. P. Broida, Phys. Rev. Letters 15, 608 (1965).

[4]M. Lipeles, R. Novick, and N. Tolk, Phys. Rev. Letters 15, 815 (1965).

[5]N. Tolk, Ph.D. thesis, Columbia U., 1966 (unpublished).

[6]S. Dworetsky, R. Novick, W. W. Smith, and N. Tolk, Phys. Rev. Letters 18, 939 (1967).

[7]D. C. Lorents and J. R. Peterson, Stanford Research Institute Project Report No. PAU 5962, 1966 (unpublished).

[8]J. H. Moore, Jr. and J. P. Doering, Phys. Rev. 174, 178 (1968).

[9]J. P. Doering, Bull. Am. Phys. Soc. 13, 204 (1968).

[10]J. H. Moore, Jr. and J. P. Doering, Phys. Rev. 177, 218 (1969).

[11]M. Lipeles, Bull. Am. Phys. Soc. 14, 632 (1969).

[12]G. H. Dunn, R. Geballe, and D. Pretzer, Phys. Rev. 128, 2200 (1962).

[13]B. Van Zyl, D. Jaecks, D. Pretzer, and R. Geballe, Phys. Rev. 136, A1561 (1964).
[14]B. Van Zyl, D. Jaecks, D. Pretzer, and R. Geballe, Phys. Rev. 158, 29 (1967).
[15]T. D. Gaily, D. H. Jaecks, and R. Geballe, Phys. Rev. 167, 81 (1968).
[16]S. H. Neff and N. P. Carleton in *Atomic Collision Processes*, edited by M. R. C. McDowell (North-Holland, Amsterdam, 1964), p. 652.
[17]R. A. Young, R. F. Stebbings, and J. William McGowan, Phys. Rev. 171, 85 (1968).
[18]C. B. Liu, Ph.D. dissertation, U. of California, Santa Barbara, 1969 (unpublished).
[19]N. G. Utterback and G. H. Miller, Rev. Sci. Instr. 32, 1101 (1961).
[20]N. G. Utterback, Phys. Rev. 129, 219 (1963).
[21]M. G. Belanger and E. A. Soltysik, J. Chem. Phys. 50, 1900 (1969).
[22]D. Krause, Jr. and E. A. Soltysik, Phys. Rev. 175, 142 (1968).
[23]N. G. Utterback and B. Van Zyl, Phys. Rev. Letters 20, 1021 (1968).
[24]D. C. Jain and R. C. Sahni, J. Quant. Spectry. Radiative Transfer 6, 705 (1966).
[25]J. P. Doering, Phys. Rev. 133, A1537 (1964).
[26]D. T. Stewart, Proc. Phys. Soc. (London) 69, 437 (1956).
[27]W. F. Sheridan, O. Oldenberg, and N. P. Carleton, *Second International Conference on the Physics of Electronic and Atomic Collisions (Abstracts)* (Benjamin, New York, 1961), p. 159.
[28]R. F. Holland, Los Alamos Scientific Laboratory Report No. LA-3783, 1967 (unpublished).
[29]J. W. McConkey and I. D. Latimer, Proc. Phys. Soc. (London) 86, 463 (1965).
[30]J. W. McConkey, J. M. Woolsey, and D. J. Burns, Planetary Space Sci. 15, 1332 (1967).
[31]B. N. Srivastava and I. M. Mirza, Phys. Rev. 168, 86 (1968).
[32]J. M. Sluyters and J. Kistemaker, Physica 25, 1389 (1959).

PHYSICAL REVIEW A VOLUME 2, NUMBER 5 NOVEMBER 1970

Range-Energy Relation in Hydrogen†

P. H. Garbincius*
Manhattan College, Bronx, New York 10471
and
L. G. Hyman
Argonne National Laboratory, Argonne, Illinois 60439
(Received 15 June 1970)

The mean excitation potential of liquid hydrogen has been determined to be 20.4 ± 0.9 eV. This value was obtained from measurement in a hydrogen bubble chamber of (i) the range of monoenergetic muons and (ii) the range and momentum of protons which stop in the chamber.

I. INTRODUCTION

The study of penetration of charged particles in matter has been of interest since the earliest experiments in nuclear physics. Such studies have intrinsic physics interest and in addition precise information on the range-energy relation can be used in the measurement of fundamental quantities such as particle masses.[1]

In the present experiment we have obtained accurate data in the Argonne National Laboratory–Midwestern Universities Research Association 30-in. hydrogen bubble chamber on the range of monoenergetic μ^+ mesons which result from the decay $\pi^+ \rightarrow \mu^+ + \nu_\mu$. We have also used measurements in the same chamber of the elastic reaction

$$\bar{p} + p \rightarrow \bar{p} + p \,, \tag{1}$$

with the outgoing proton stopping in the chamber. The $\bar{p}p$ measurements were made on POLLY,[2] which is a cathode-ray tube device at Argonne which scans and precisely measures bubble-chamber film.

The density of H_2 in the bubble chamber was deduced from the operating conditions and was combined with the muon length measurement and the proton measurements to give a best estimate of I, the mean excitation energy in the Bethe-Bloch equation.[3]

II. THEORY

A basic expression for energy loss per unit path length of a charged particle in passing through matter is given by the Bethe-Bloch equation

$$-\frac{\partial E}{\partial X} = \frac{2\pi z^2 e^4 NZ}{mc^2\beta^2 A}\left(\ln\frac{2mc^2\gamma^2\beta^2 Q_{\max}}{I^2} - 2\beta^2 - \frac{2C}{Z} - \delta\right) , \tag{2}$$

where $Q_{\max}$ is the maximum energy that can be transferred per collision and is given by

$$Q_{\max} = 2mc^2\gamma^2\beta^2/[1 + (2\gamma m/M) + (m/M)^2] \quad .$$